SUPPORTING INFORMATION

Ferric Heme Superoxide Reductive Transformations to Ferric Heme (Hydro)Peroxide Species: Spectroscopic Characterization and Thermodynamic Implications for H-atom Transfer (HAT)

Hyun Kim,[†] Patrick J. Rogler,[†] Savita K. Sharma,[†] Andrew W. Schaefer,[‡] Edward I. Solomon,*[‡] and Kenneth D. Karlin*[†]

[†]Department of Chemistry, Johns Hopkins University, Baltimore, Maryland 21218, United States
[‡]Department of Chemistry, Stanford University, Stanford, California 94305, United States

To whom correspondence should be addressed. E-mail: solomone@stanford.edu, karlin@jhu.edu

1. Materials and Methods.

All reagents and solvents purchased and used were of commercially available quality except as noted. Inhibitor-free Tetrahydrofuran (THF) was distilled over Na/benzophenone under argon and deoxygenated with argon before use. Butyronitrile was distilled over sodium carbonate and potassium permanganate and deoxygenated with Ar before use. Cobaltocene was obtained from Sigma Aldrich, sublimed at 75°C, and stored under nitrogen in the glovebox freezer at –30 °C. The 2,6-lutidinium Triflate [(Lu)(H)](OTf), TEMPO-H, and ABNO-H were synthesized according to previously published literature procedures.[1–3]

The preparation and handling of air-sensitive compounds were performed under a MBraun Labmaster 130 inert atmosphere (< 1 ppm O_2 and < 1 ppm H_2O) glovebox filled with nitrogen. Dioxygen gas purchased from Airgas and dried through Drierite. $^{18}O_2$ gas was purchased from ICON, Summit, NJ, and $^{16}O_2$ gas was purchased from BOC gases, Murray Hill, NJ.

All UV−vis measurements were carried out as previously described[4,5] using a Hewlett-Packard 8453 diode array spectrophotometer with HP Chemstation software and a Unisoku thermostated cell holder for low-temperature experiments. A 10 mm path length quartz cell cuvette modified with an extended glass neck with a female 14/19 joint, and stopcock was used to perform all UV–vis experiments, as previously described.[5–7] ^{1}H NMR spectra were measured on a Bruker 300-MHz NMR spectrometer at ambient or low temperatures. Chemical shifts were reported as δ (ppm) values relative to an internal standard (tetramethylsilane) and the residual solvent proton peaks. Electron paramagnetic resonance (EPR) spectra were recorded with a Bruker EMX spectrometer equipped with a Bruker ER 041 × G microwave bridge and a continuous flow liquid helium cryostat (ESR900) coupled to an Oxford Instruments TC503 temperature controller. Spectra were obtained at 10 K under non-saturating microwave power conditions (ν = 9.428 GHz, microwave power = 0.201 mW, modulation amplitude = 10 G, microwave frequency = 100 kHz, and receiver gain = 5.02 × 10^3).

The compound $(P^{Im})Fe^{II}$ was synthesized as previously described.[4]

2. UV-vis Spectroscopy.

Generation of $[(P^{Im})Fe^{III}–(O_2^{2–})]$ (P^{Im}-*P*). In an inert atmosphere glovebox, a 0.05 mM solution of $[(P^{Im})Fe^{II}]$ was prepared in THF in a 2 mm path length quartz Schlenk cuvette capped with a rubber septum. The cuvette was cooled in the cryostat chamber to –80 ℃. Dioxygen was bubbled through the solution, and excess O_2 was purged out of the tubes by bubbling with Ar. Then, 15 µL (3 equiv) of a 10 mM solution of $CoCp_2$ dissolved in butyronitrile were added via gastight syringe to the solution of $[(P^{Im})Fe^{III}–(O_2^{\bullet-})]$ (**P^{Im}-*S***) and mixed by bubbling with Ar in THF at –80 ℃. UV-vis: λ_{max} = 424, 535, and 567 nm.

Generation of $[(P^{Im})Fe^{III}–(OOH)]$ (P^{Im}-*HP*). After generating complex $[(P^{Im})Fe^{III}–(O_2^{2–})]^–$ (**P^{Im}-*P***) as described above, 10 µL (1 equiv) of a 5 mM solution of $[(LutH^+)](OTf)$ dissolved in THF was added via gastight syringe to the solution of **P^{Im}-*P*** and mixed by bubbling with Ar in THF at –80 ℃. UV-vis: λ_{max} = 423 and 533 nm.

H_2O_2 Quantification by Horseradish Peroxidase (HRP) Test. The spectrophotometric quantification of hydrogen peroxide was carried out by analyzing the intensity of the diammonium 2,2′-azino-bis(3-ethylbenzothiazoline-6-sulfonate)(AzBTS-$(NH_4)_2$) peaks (at different wavelengths to minimize error, Figure S1), which was oxidized by horseradish peroxidase (HRP); this was adapted from published procedures.[8,9] Three stock solutions were prepared: 300 mM

sodium phosphate buffer pH 7.0 (solution A), 1 mg/mL AzBTS-$(NH_4)_2$ (solution B) and 4 mg of HRP (type II salt free (Sigma)) with 6.5 mg of sodium azide in 50 mL of water (solution C). 3.0 mL of the desired [$(P^{Im})Fe^{III}$–(O_2^{2-})] (**P^{Im}-*P***) or [$(P^{Im})Fe^{III}$–(OOH)] (**P^{Im}-*HP***) solution were generated in THF at –80 ℃, as previously described. The reaction which is before and after being quenched by adding 100μL of triflic acid (HOTf) solution (2.5 equiv) is subject to the H_2O_2 analysis. Subsequently 100 μL of the cold THF sample solution was removed via a syringe and quickly added to a cuvette containing 1.3 mL of water, 500 μL of solution A, 100 μL of solution B, and 50 μL of solution C (all chilled in an ice bath prior to use). After mixing for 15s, the samples were allowed to sit at room temperature for ~2 min until full formation of the 418 nm band was observed (Figure S1).

Determination of the reduction potential of [$(P^{Im})Fe^{III}$–(O_2^{2-})] (P^{Im}-*P*). In a 2mm path length quartz Schlenk cuvette, [$(P^{Im})Fe^{III}$–$(O_2^{\bullet-})$] (**P^{Im}-*S***) was generated as previously published.[4] Titrations of 0.25–3 equiv $CoCp_2$ dissolved in butyronitrile were carried out in THF at –80 ℃. For each equilibrium mixture, the concentration of each species in solution was measured using the absorption at either 423 or 567 nm (Table S1). From these equilibrium constants, corresponding reduction potentials were calculated by using the Nernst equation.

Reversibility of [$(P^{Im})Fe^{III}$–$(O_2^{\bullet-})$] (P^{Im}-*S*) and [$(P^{Im})Fe^{III}$–(O_2^{2-})] (P^{Im}-*P*). In a 2 mm path length quartz Schlenk cuvette, 1 equiv ferrocenium prepared in a glovebox was added via gastight syringe to a solution of [$(P^{Im})Fe^{III}$–(O_2^{2-})] (**P^{Im}-*P***) generated from [$(P^{Im})Fe^{III}$–$(O_2^{\bullet-})$] (**P^{Im}-*S***) with 3 equiv $CoCp_2$ in THF at –80 ℃. Then, excess amount of $CoCp_2$ was added to this resulting solution via gastight syringe (Figure S4).

Determination of the pK_a of [$(P^{Im})Fe^{III}$–(OOH)] (P^{Im}-*HP*). In a 2 mm path length quartz Schlenk cuvette, [$(P^{Im})Fe^{III}$–(OOH)] (**P^{Im}-*HP***) was generated as described above. Titrations of 0.25–2 equiv EtP_2(dma) prepared in a glovebox were carried out in THF at –80 ℃. For each equilibrium mixture, the concentration of each species in solution was measured using the absorption at either 423 or 567 nm (Table S2). From these equilibrium constants, the pK_a was calculated.

Reversibility of [$(P^{Im})Fe^{III}$–(O_2^{2-})]$^-$ (P^{Im}-*P*) and [$(P^{Im})Fe^{III}$-(OOH)] (P^{Im}-*HP*). In a 2 mm path length quartz Schlenk cuvette, 2 equiv EtP_2(dma) prepared in a glovebox was added via gastight syringe to a solution of [$(P^{Im})Fe^{III}$–(OOH)] (**P^{Im}-*HP***) generated as described above. Then, 3 equiv [$(LutH^+)$](OTf) was added to this resulting solution via gastight syringe (Figure S8).

3. Electron Paramagnetic Resonance (EPR) Spectroscopy.

In a glovebox, 1 mM solutions of $(P^{Im})Fe^{II}$ in THF were prepared and transferred to EPR tube and capped with tightfitting septum. The sample tubes were placed in a cold bath (dry ice/acetone) and then O_2 was bubbled through the solution. The excess O_2 was purged out of the tubes by bubbling with Ar, and then the oxygenated samples were set in a cold bath for 10 min. The solution of $CoCp_2$ dissolved in butyronitrile in a glovebox was added via gastight syringe to the solution of [$(P^{Im})Fe^{III}$–$(O_2^{\bullet-})$] (**P^{Im}-*S***). Subsequently, 1 equiv [$(LutH^+)$](OTf) was added via gastight syringe, followed by mixing of the solution by bubbling Ar, for complex [$(P^{Im})Fe^{III}$–(OOH)] (**P^{Im}-*HP***). Then, the sample tubes were frozen in liquid N_2.

For EPR data for the reaction of [$(P^{Im})Fe^{III}$–$(O_2^{\bullet-})$] (**P^{Im}-*S***) with TEMPO–H, 10 equiv TEMPO–H prepared in a glovebox was added via gastight syringe to the 1mM solution of **P^{Im}-*S*** generated as described above. The tube was left at –80 ℃ for 1 hour 30 minutes and then frozen in liquid nitrogen and sealed by flame.

4. Resonance Raman Spectroscopy.

In the glovebox, 1 mM solutions of $(P^{Im})Fe^{II}$ in THF were prepared and transferred to rR tube and capped with tightfitting septum. The sample tubes were placed in a cold bath (dry ice/acetone) and then either $^{16}O_2$ or $^{18}O_2$ gas was bubbled through the solution. The excess either $^{16}O_2$ or $^{18}O_2$ was purged out of the tubes by bubbling with Ar, and then the oxygenated samples were set in a cold bath for 10 min. The solution of $CoCp_2$ dissolved in butyronitrile in a glovebox was added via gastight syringe to the solution of $[(P^{Im})Fe^{III}–(O_2^{\bullet-})]$ (**P^{Im}-*S***). Subsequently, 1 equiv $[(LutH^+)](OTf)$ was added via gastight syringe, followed by mixing of the solution by bubbling Ar, for complex $[(P^{Im})Fe^{III}–(OOH)]$ (**P^{Im}-*HP***). Then, the sample tubes were frozen in liquid N_2. Resonance Raman samples were excited at 413 nm, using a Coherent I90C-K Kr^+ ion laser while the sample was immersed in a liquid nitrogen cooled (77 K) EPR finger Dewar (Wilmad). Power was ~2 mW at the sample, which was continuously rotated to minimize photodecomposition. The spectra were recorded using a Spex 1877 CP triple monochromator, and detected by an Andor Newton CCD cooled to –80 °C.

5. Calculations for the determination of the reduction potential of [(P^{Im})Fe^{III}–($O_2^{\bullet-}$)] (P^{Im}-***S***) and pK_a of [(P^{Im})Fe^{III}–(OOH)] (P^{Im}-***HP***)

Table S1. Equilibrium concentrations for the titration of $CoCp_2$ into a solution of [(P^{Im})Fe^{III}–($O_2^{\bullet-}$)] (**P^{Im}-*S***) in THF at –80 °C

At 567 nm

$[CoCp_2]_{added}$	$[CoCp_2]_{eq}$	$[Peroxide]_{eq}$	$[Superoxide]_{eq}$	$[CoCp_2]^+_{eq}$	K_{eq}	Es (mV)
4.98×10^{-5}	3.00×10^{-5}	1.98×10^{-5}	8.02×10^{-5}	1.98×10^{-5}	1.63×10^{-1}	–1.36
9.88×10^{-5}	3.98×10^{-5}	5.90×10^{-5}	4.10×10^{-5}	5.90×10^{-5}	2.13	–1.32
1.47×10^{-4}	7.30×10^{-5}	7.41×10^{-5}	2.59×10^{-5}	7.41×10^{-5}	2.90	–1.31
1.95×10^{-4}	1.09×10^{-4}	8.51×10^{-5}	1.49×10^{-5}	8.51×10^{-5}	4.46	–1.31
2.41×10^{-4}	1.51×10^{-4}	9.07×10^{-5}	9.29×10^{-6}	9.07×10^{-5}	5.88	–1.30

At 423 nm

$[CoCp_2]_{added}$	$[CoCp_2]_{eq}$	$[Peroxide]_{eq}$	$[Superoxide]_{eq}$	$[CoCp_2]^+_{eq}$	K_{eq}	Es (mV)
5.00×10^{-5}	4.04×10^{-5}	9.64×10^{-6}	4.04×10^{-5}	9.64×10^{-5}	5.71×10^{-2}	–1.38
9.95×10^{-5}	8.23×10^{-5}	1.72×10^{-5}	3.28×10^{-5}	1.72×10^{-5}	1.09×10^{-1}	–1.37
1.48×10^{-4}	1.20×10^{-5}	2.87×10^{-5}	2.13×10^{-5}	2.87×10^{-5}	3.24×10^{-1}	–1.35
2.45×10^{-4}	1.57×10^{-4}	3.97×10^{-5}	1.03×10^{-5}	3.97×10^{-5}	9.78×10^{-1}	–1.33
2.92×10^{-4}	1.99×10^{-4}	4.59×10^{-5}	4.07×10^{-6}	4.59×10^{-5}	2.61×10^{-1}	–1.31

$$E = E^{\circ\prime} - (RT/nF)\ln(Q) \quad \text{(S1)}$$

$$0 = E^{\circ\prime} - (RT/nF)\ln(K_{eq}) \quad \text{(S2)}$$

$$E^{\circ\prime} = E_S - E_{Co} \quad \text{(S3)}$$

$$E_S = E_{Co} + (RT/nF)\ln(K_{eq}) \quad \text{(S4)}$$

E is the potential of the system, which is zero at equilibrium. R is the gas constant (8.314 J/K•mol), T is the temperature (193.15 K), n is the number of electrons (1), F is Faraday's constant (96485.33 C/mol), E_{Co} is the reduction potential of $CoCp_2$ (–1.33 V vs $Fc^{+/0}$ in THF), K_{eq} is the equilibrium constant (values given in Table S1), and E_S is the reduction potential of the [(P^{Im})Fe^{III}–($O_2^{\bullet-}$)] (**P^{Im}-*S***).

Table S2. Equilibrium concentrations for the titration of $EtP_2(dma)$ into a solution of $[(P^{Im})Fe^{III}–(OOH)]$ (**P^{Im}-*HP***) in THF at –80 °C

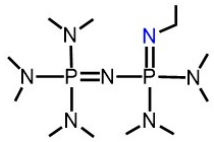

At 567 nm

$[EtP_2(dma)]_{added}$	$[Peroxide]_{eq}$	$[EtP_2(dma)]_{eq}$	$[Hydroperoxide]_{eq}$	$[EtP_2(dma)H^+]_{eq}$	K_{eq}	pK_{eq}	pK_a
2.41×10^{-5}	1.05×10^{-5}	1.35×10^{-5}	8.61×10^{-5}	1.05×10^{-5}	0.09	1.02	27.1
4.79×10^{-5}	3.81×10^{-5}	9.79×10^{-6}	5.84×10^{-5}	3.81×10^{-5}	2.54	–0.40	28.5
7.16×10^{-5}	6.08×10^{-5}	1.08×10^{-5}	3.58×10^{-5}	6.07×10^{-5}	9.48	–0.97	29.1
9.51×10^{-5}	7.52×10^{-5}	1.99×10^{-5}	2.14×10^{-5}	7.52×10^{-5}	13.2	–1.12	29.2
1.41×10^{-4}	9.02×10^{-5}	5.13×10^{-4}	6.35×10^{-6}	9.02×10^{-5}	24.9	–1.39	29.5

At 423 nm

$[EtP_2(dma)]_{added}$	$[Peroxide]_{eq}$	$[EtP_2(dma)]_{eq}$	$[Hydroperoxide]_{eq}$	$[EtP_2(dma)H^+]_{eq}$	K_{eq}	pK_{eq}	pK_a
2.5×10^{-5}	1.06×10^{-5}	1.43×10^{-5}	3.74×10^{-5}	1.06×10^{-5}	0.21	0.67	27.4
4.95×10^{-5}	1.81×10^{-5}	3.14×10^{-5}	2.99×10^{-5}	1.81×10^{-5}	0.34	0.45	27.6
7.35×10^{-5}	3.13×10^{-5}	4.21×10^{-5}	1.67×10^{-5}	3.13×10^{-5}	1.39	–0.14	28.2
9.71×10^{-5}	4.48×10^{-5}	5.23×10^{-5}	3.25×10^{-5}	4.48×10^{-5}	11.7	–1.07	29.2

$$pK_a^{THF}(\text{Hydroperoxide}) = pK_a^{THF}(EtP_2(dma)) - pK_{eq} \quad \text{(S5)}$$

As shown by a titration of UV-vis spectroscopy at 567 nm in Figure 4B, the absorption band at 567 nm of $[(P^{Im})Fe^{III}–(O_2^{2–})]^–$ (**P^{Im}-*P***) increased with increasing concentration of added $EtP_2(dma)$. The UV-vis absorptions for (**P^{Im}-*P***) and $[(P^{Im})Fe^{III}–(OOH)]$ (**P^{Im}-*HP***) gave direct determination (since we know the spectrum and absorptivities of the compound in their pure form) of their concentrations, thus defining the amount/concentration of $EtP_2(dma)$ reacted and of $[EtP_2(dma)]H^+$ formed.

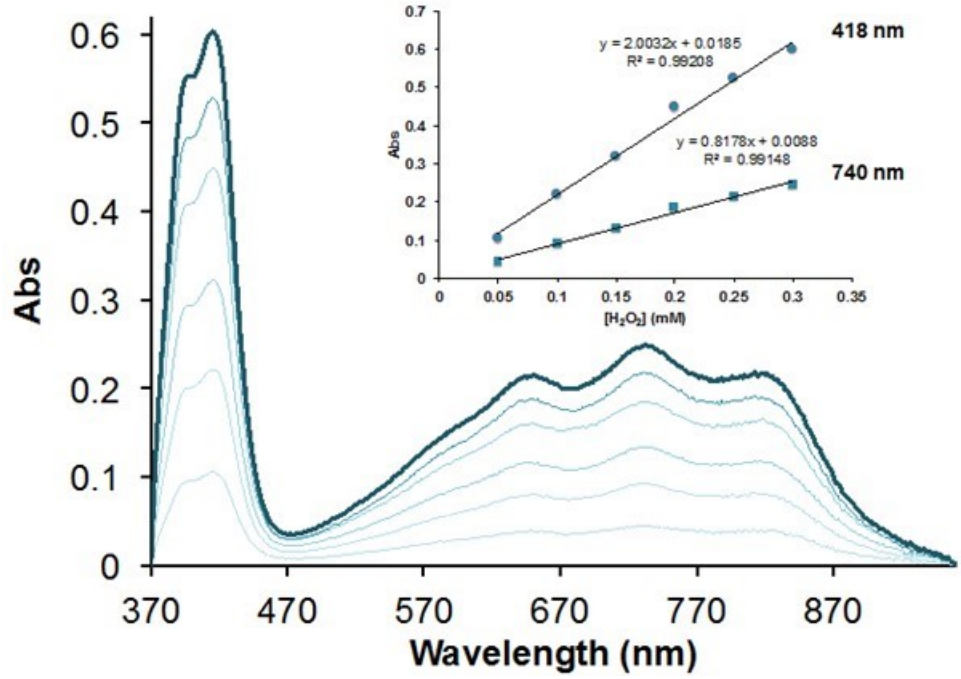

Figure S1. Calibration curve (adapted from ref 9) used for H_2O_2 quantification by the horseradish peroxidase (HRP) test. See experimental description (above) for details.[8,9]

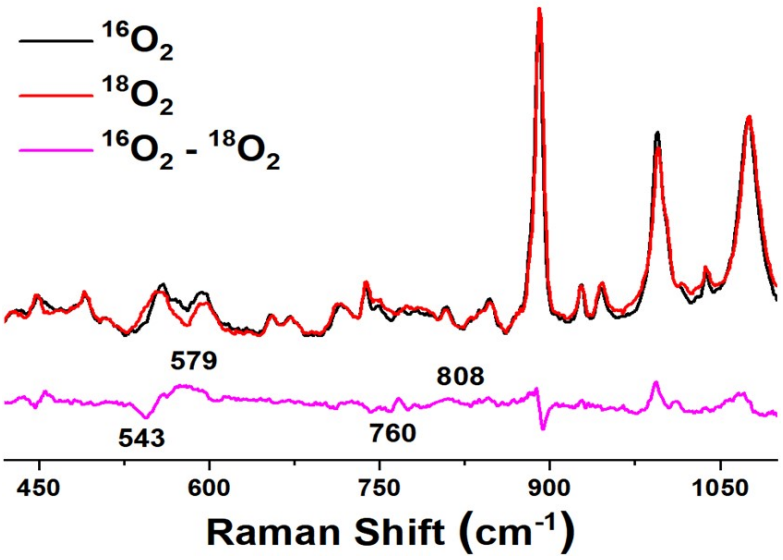

Figure S2. Resonance Raman spectra of ferric heme hydroperoxide complex [(P^{Im})Fe^{III}–(OOH)] (**P^{Im}-*HP***) in frozen THF obtained at 77 K with 413 nm excitation.

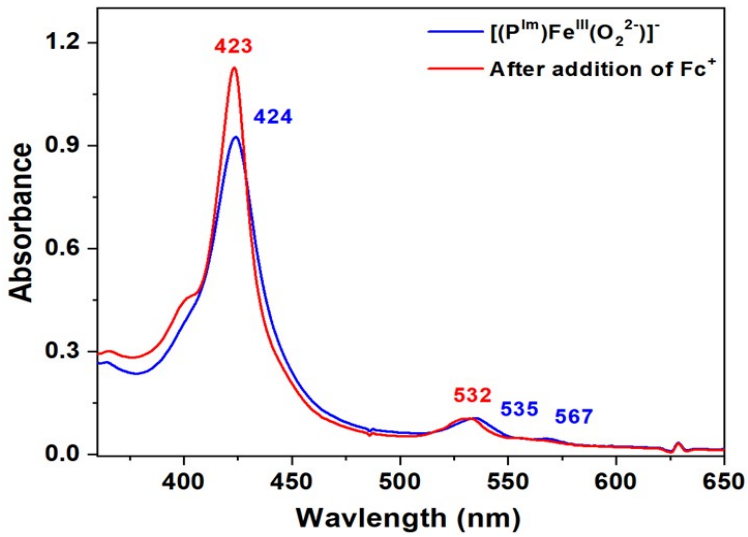

Figure S3. UV–vis spectra demonstrating the oxidation of $[(P^{Im})Fe^{III}–(O_2^{2–})]^–$ (**P^{Im}-*P***) to form $[(P^{Im})Fe^{III}–(O_2^{\bullet–})]$ (**P^{Im}-*S***) at –80 ℃ in THF.

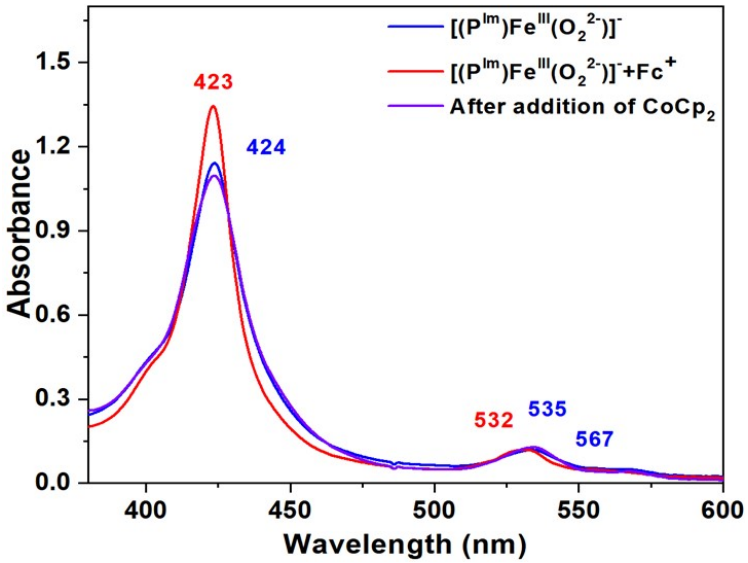

Figure S4. Addition of 1 equivalent of ferrocenium to $[(P^{Im})Fe^{III}–(O_2^{2–})]^–$ (**P^{Im}-*P***) (blue) regenerates the formation of $[(P^{Im})Fe^{III}–(O_2^{\bullet–})]$ (**P^{Im}-*S***) (red) and again, upon addition of excess amount of $CoCp_2$, to this resulting solution, $[(P^{Im})Fe^{III}–(O_2^{2–})]^–$ (**P^{Im}-*P***) (purple) is formed.

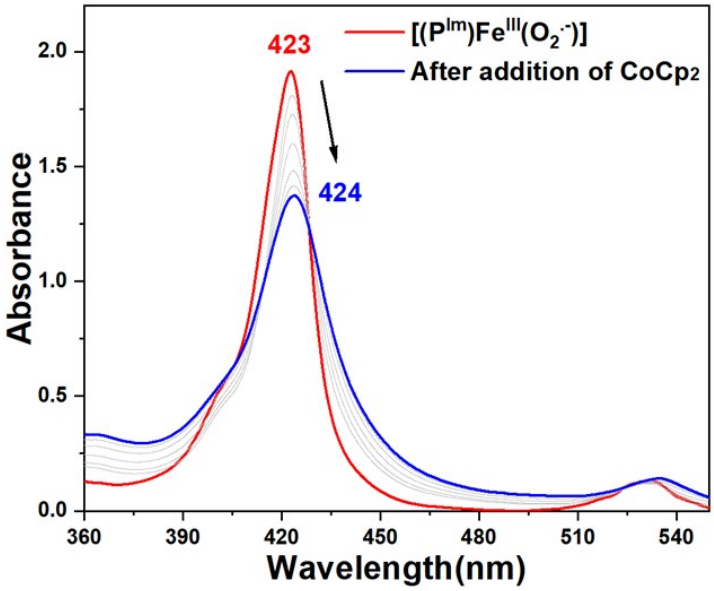

Figure S5. UV-vis spectroscopic monitoring of the incremental addition of $CoCp_2$ to a solution of $[(P^{lm})Fe^{III}–(O_2^{\bullet-})]$ (**P^{lm}-*S***).

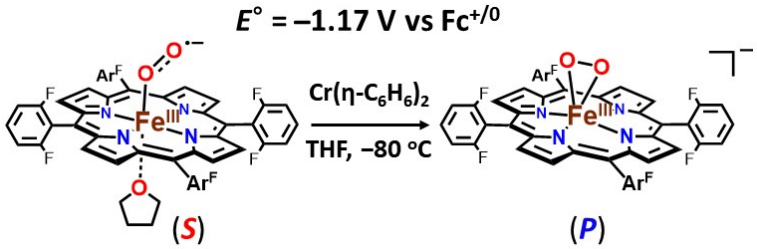

Figure S6. The reduction potential of $[(F_8)Fe^{III}–(O_2^{\bullet-})]$ (***S***)/ $[(F_8)Fe^{III}–(O_2^{2-})]^-$ (***P***) couple was calculated to be –1.17 V vs $Fc^{+/0}$ in THF.[10]

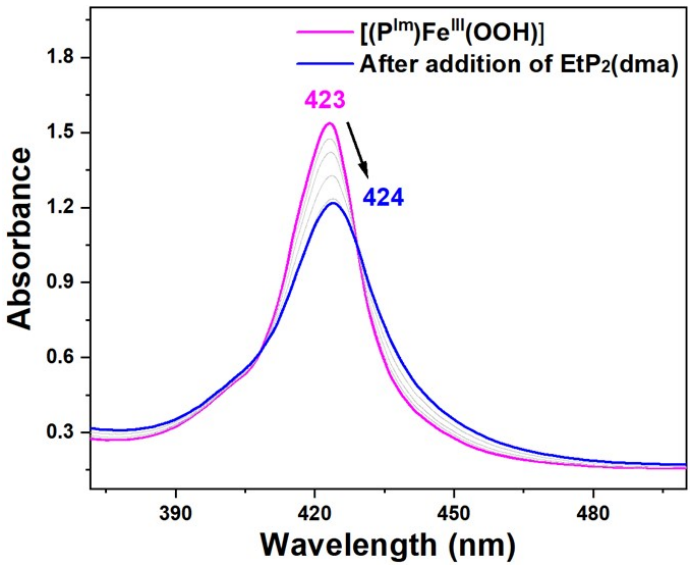

Figure S7. Conversion of [(P^{Im})Fe^{III}–(OOH)] (**P^{Im}-*HP***) (pink) to [(P^{Im})Fe^{III}–(O_2^{2-})]$^-$ (**P^{Im}-*P***) (blue) upon addition of EtP$_2$(dma) at –80 °C in THF, resulting in the generation of equilibrium mixtures which allowed the determination of the pK_a of the **P^{Im}-*HP***.

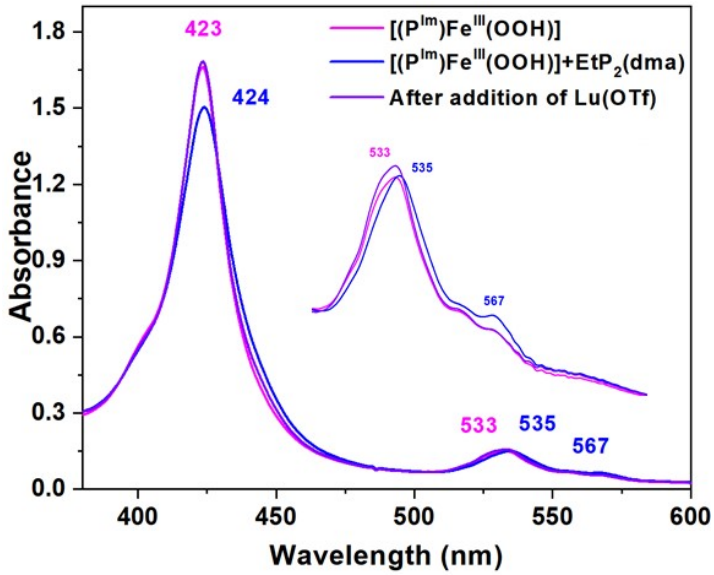

Figure S8. Addition of EtP$_2$(dma) to the solution of [(P^{Im})Fe^{III}–(OOH)] (**P^{Im}-*HP***) (pink) regenerates complex [(P^{Im})Fe^{III}–(O_2^{2-})]$^-$ (**P^{Im}-*P***) (blue). This resulting solution can be protonated again to form complex **P^{Im}-*HP*** (purple) by adding [(LutH$^+$)](OTf).

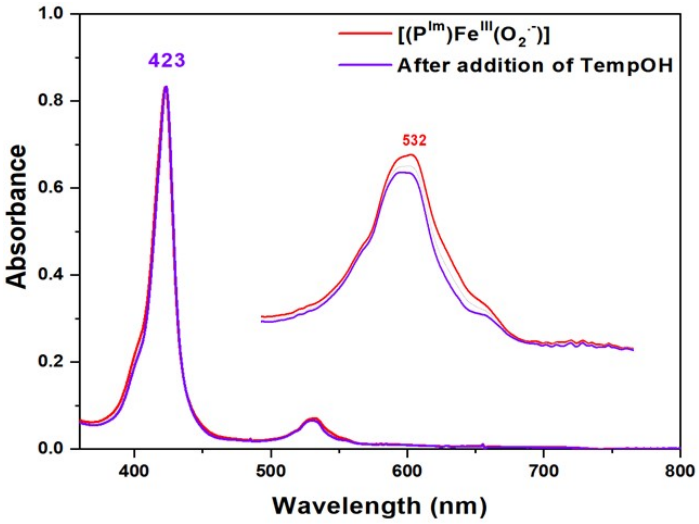

Figure S9. UV-vis spectra monitoring the reaction of [(P^{lm})Fe^{III}–($O_2^{\bullet-}$)] (**P^{lm}-*S***) with TEMPO-H at –80 ℃ in THF.

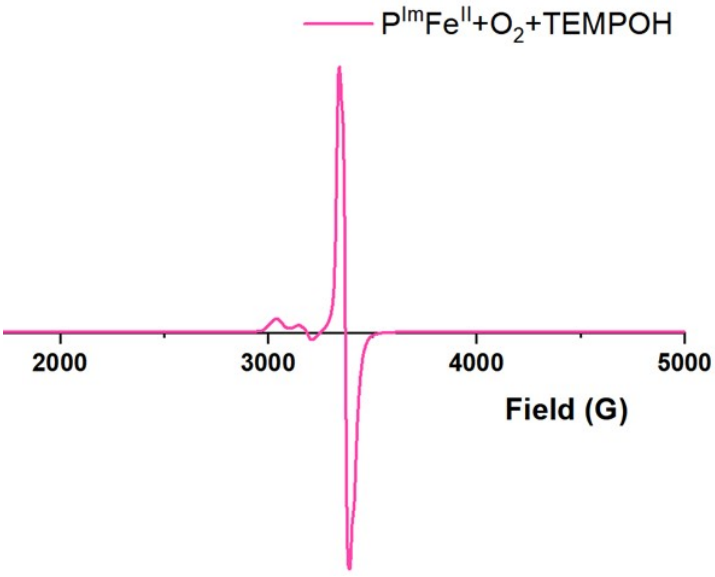

Figure S10. EPR spectrum of the reaction of [(P^{lm})Fe^{III}–($O_2^{\bullet-}$)] (**P^{lm}-*S***) with TEMPO-H in frozen THF. Spin quantification of the EPR signal shows that the yield of the TEMPO radical is 94%.

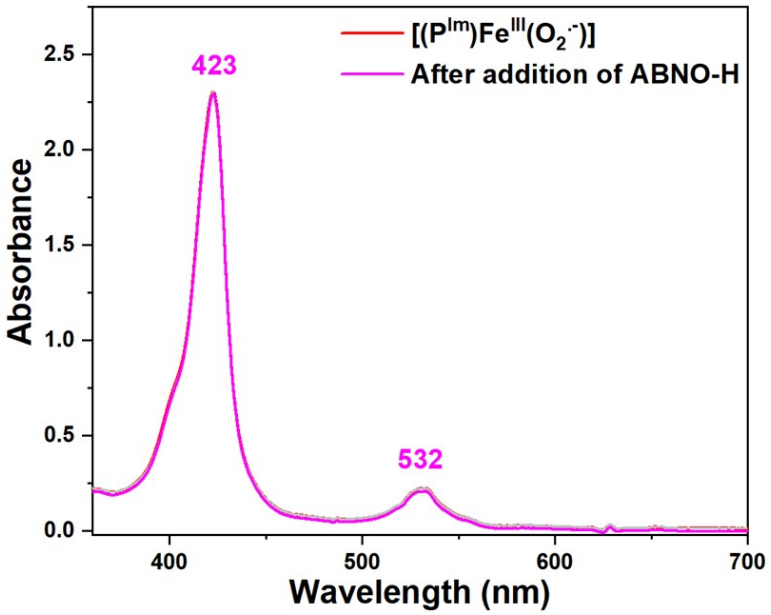

Figure S11. UV-vis spectroscopy following the addition of ABNO-H to the solution of [(P^{lm})Fe^{III}–($O_2^{\bullet-}$)] (**P^{lm}-*S***) in THF at −80 °C. No reaction is observed.

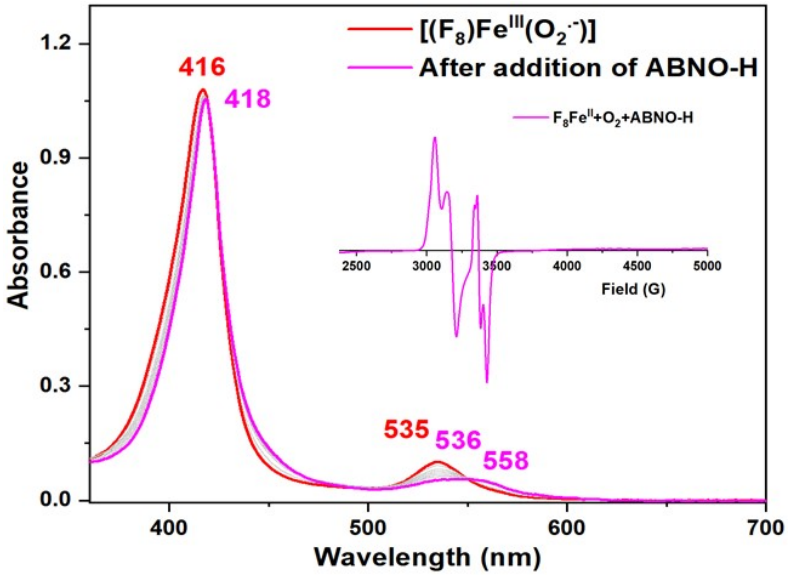

Figure S12. UV−vis spectroscopic monitoring the reaction of [(F_8)Fe^{III}–($O_2^{\bullet-}$)] (***S***) (red) with ABNO-H in THF at −80 °C to yield [(F_8)Fe^{III}–(OOH)] (***HP***) (pink). Inset: 10 K EPR spectrum of the final products of ABNO-H HAT by ***S*** in frozen THF. Spin quantification reveals that the EPR signal corresponds to ~68% yield of ***S***, but the yield of ABNO radical is low probably due to side-reactions, yet showing the expected triplet features (at g = 2; Inset). The overall time for the reaction to reach completion is ~5.0 hours.

6. References

[1] J. J. Curley, R. G. Bergman, T. D. Tilley, *Dalt. Trans.* **2012**, *41*, 192–200.

[2] E. A. Mader, E. R. Davidson, J. M. Mayer, *J. Am. Chem. Soc.* **2007**, *129*, 5153–5166.

[3] T. R. Porter, D. Capitao, W. Kaminsky, Z. Qian, J. M. Mayer, *Inorg. Chem.* **2016**, *55*, 5467–5475.

[4] Y. Li, S. K. Sharma, K. D. Karlin, *Polyhedron* **2013**, *58*, 190–196.

[5] S. K. Sharma, A. W. Schaefer, H. Lim, H. Matsumura, P. Moënne-Loccoz, B. Hedman, K. O. Hodgson, E. I. Solomon, K. D. Karlin, *J. Am. Chem. Soc.* **2017**, *139*, 17421–17430.

[6] R. A. Ghiladi, H.-W. Huang, P. Moënne-Loccoz, J. Stasser, N. J. Blackburn, A. S. Woods, R. J. Cotter, C. D. Incarvito, A. L. Rheingold, K. D. Karlin, *J. Biol. Inorg. Chem.* **2005**, *10*, 63–77.

[7] I. M. Wasser, H.-w. Huang, P. Moënne-Loccoz, K. D. Karlin, *J. Am. Chem. Soc.* **2005**, *127*, 3310–3320.

[8] R. L. Peterson, J. W. Ginsbach, R. E. Cowley, M. F. Qayyum, R. A. Himes, M. A. Siegler, C. D. Moore, B. Hedman, K. O. Hodgson, S. Fukuzumi, E. I. Solomon, K. D. Karlin, *J. Am. Chem. Soc*. **2013**, *135*, 16454–16467.

[9] S. M. Adam, I. Garcia-Bosch, A. W. Schaefer, S. K. Sharma, M. A. Siegler, E. I. Solomon, K. D. Karlin, *J. Am. Chem. Soc*. **2017**, *139*, 472–481.

[10] H. Kim, P. J. Rogler, S. K. Sharma, A. W. Schaefer, E. I. Solomon, K. D. Karlin, *J. Am. Chem. Soc*. **2020**, *142*, 3104–3116.